JOC Article

# Taking Advantage of the Radical Character of Tris(2,4,6-trichlorophenyl)methyl To Synthesize New Paramagnetic Glassy Molecular Materials

Sonia Castellanos,[†] Dolores Velasco,[‡] Francisco López-Calahorra,[‡] Enric Brillas,[§] and Luis Julia*,[†]

*Departament de Química Orgànica, Institut de Nanociències I Nanotecnologia, Universitat de Barcelona, Martí i Franquès 1-11, 08028 Barcelona, Spain, Departament de Química Orgànica Biològica, Institut d'Investigacions Químiques i Ambientals (CSIC), Jordi Girona 18-26, 08034 Barcelona, Spain, and Departament de Química Física, Universitat de Barcelona, Martí i Franquès 1-11, 08028 Barcelona, Spain*

*ljbmoh@cid.csic.es*

*Received December 21, 2007*

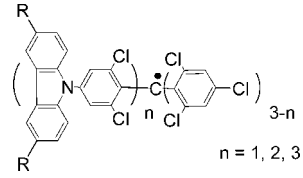


This paper describes the synthesis of the novel bis[4-(*N*-carbazolyl)-2,6-dichlorophenyl](2,4,6-trichlorophenyl)methyl radical (**2**•) and tris[4-(*N*-carbazolyl)-2,6-dichlorophenyl]methyl radical (**3**•). A Friedel−Crafts reaction on [4-(*N*-carbazolyl)-2,6-dichlorophenyl)bis(2,4,6-trichlorophenyl]methyl radical (**1**•), **2**•, and **3**• leads to the introduction of acyl chains in the 3- and 6-positions of the carbazolyl moiety without impairment of the radical character of the molecule to give radicals **5**•, **6**•, and **7**•. All of these novel radical adducts are thermally stable, **5**• and **6**• being amorphous solids by differential scanning calorimetry. Electron paramagnetic resonance spectra of them show a multiplet at low temperature due to the electron-coupling with six aromatic hydrogens. They show electrochemical amphotericity being reduced and oxidized to their corresponding stable anionic and cationic species, respectively. These radical adducts have luminescent properties covering the red spectral band of the emission with high intensities.

## Introduction

Carbazole derivatives are of great interest for their optical and redox properties. They show relatively intense luminescence[1] and undergo reversible oxidation processes to stable radical cations, making them good hole carriers with a positive charge.[2] As good materials for organic light-emitting diodes (OLED), carbazoles are used for hole-transporting and light-emitting layers.[3] In addition, carbazole as a constituent of polymers can greatly improve the photoconductivities and hole-transporting properties of them.[4] Many of these materials are stable amorphous glasses above room temperature and have advantages over crystalline materials because they can form uniform and transparent amorphous films by spin coating, solvent casting from solution, and vacuum deposition.[5]

Recently, we have reported the synthesis and properties of the (4-*N*-carbazolyl-2,6-dichlorophenyl)bis(2,4,6-trichlorophenyl)methyl radical (**1**•),[6] resulting from the coupling of the *N*,*H*-carbazole to the tris(2,4,6-trichlorophenyl)methyl (TTM) radical. This new crystalline paramagnetic adduct with a singly occupied

[†] Institut d'Investgacions Químiques i Ambientals (CSIC).
[‡] Departament de Química Orgànica, Institut de Nanociencies i Nanotecnologia.
[§] Departament de Química Física.

(1) (a) Berlman, I. B. *Handbook of Fluorescence Spectra of Aromatic Molecules*; Academic Press: New York, 1971; p 205. (b) Mastrangelo, J. C.; Conger, B. M.; Chen, S. H.; Bashir-Hashemi, A. *Chem. Mater.* **1997**, *9*, 227–232. (c) Conger, B. M.; Katsis, D.; Mastrangelo, J. C.; Chen, S. H. *J. Phys. Chem. A* **1998**, *102*, 9213–9218. (d) Castex, M. C.; Olivero, C.; Pichler, G.; Ades, D.; Cloutet, E.; Siove, A. *Synth. Met.* **2001**, *122*, 59–61.

(2) (a) Grazulevicius, J. V.; Strohriegl, P.; Pielichowski, J.; Pielichowski, K. *Prog. Polym. Sci.* **2003**, *28*, 1297–1353. (b) Parimal, K.; Justin Thomas, K. R.; Jiann, T. L.; Tao, Y. T.; Chien, C. H. *Adv. Funct. Mater.* **2003**, *13*, 445–452. (c) Akira, B.; Ken, O.; Wolfgang, K.; Rigoberto, C. A. *J. Phys. Chem. B* **2004**, *108*, 18949–18955.

(3) (a) Adamovich, V. I.; Cordero, S. R.; Djurovich, P. I.; Tamayo, A.; Thompson, M. E.; D'Andrade, B. W.; Forrest, S. R. *Org. Electronics* **2003**, *4*, 77–87. (b) van Dijken, A.; Bastiaansen, J. J. A. M.; Kiggen, N. M. M.; Langeveld, B. M. W.; Rothe, C.; Monkman, A.; Bach, I.; Stössel, P.; Brunner, K. *J. Am. Chem. Soc.* **2004**, *126*, 7718–7727. (c) Morin, J. F.; Drolet, N.; Tao, Y.; Leclerc, M. *Chem. Mater.* **2004**, *16*, 4619–4626. (d) Justin Thomas, K. R.; Velusamy, M.; Lin, J. T.; Tao, Y. T.; Chuen, C. H. *Adv. Funct. Mater.* **2004**, *14*, 387–392.

10.1021/jo702723k CCC: $40.75 © 2008 American Chemical Society
Published on Web 04/18/2008

molecular orbital (SOMO) as the valence orbital, and high thermal stability, has interesting luminescent properties with emission in the red region of the spectrum and, consequently, with small SOMO−LUMO energy gap. It also shows attractive electrochemical properties with quasi-reversible processes either in the anodic or in the cathodic region to give cationic or anionic species, respectively, with excellent stability. As an element belonging to the series of TTM radical, the stability of radical adduct **1**• is due to the steric hindrance of six chlorine atoms around the trivalent carbon.[7,8] All of these radicals are completely disassociated (they do not dimerize) and present a large stability either in solid or in solution. They do not abstract H-atoms from hydrogen-labile species, but they are very sensitive to electron-transfer reactions, being easily reduced to anions and oxidized to cations in the presence of electron donor and acceptor species, respectively. The stability of the charged species is comparable to that of their radical precursors. Therefore, we have taken advantage of the properties afforded by the combination of the TTM radical and carbazole. It is worth mentioning that carbazole itself emits in the ultraviolet region of the spectrum and TTM radical only shows very poor luminescent properties. On the other hand, by virtue of having an unpaired electron we can obtain information using electron paramagnetic resonance (EPR) spectroscopy.

To manipulate the energy gap between the SOMO and LUMO orbitals and obtain a range of luminescence emission wavelengths into the red region, we have reported the synthesis of a series of carbazolylTTM radical adducts with electron-withdrawing or electron-donating groups in the 3- and 6-positions of the carbazole moiety.[9] Thus, a collection of new adducts with emissions between 601 and 661 nm in cyclohexane solution and between 591 and 680 nm in chloroform were described. However, the EPR spectra of all these new radical adducts appear to be practically the same without appreciable differences in spite of the presence of substituents in the carbazole ring of different nature. This is due to the fact that the spin density of these species resides mainly in the trivalent carbon atom by virtue of the presence of the bulky polychlorophenyl substituents leading to a poor spin delocalization in the molecule.

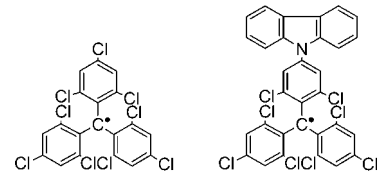


This paper reports the synthesis and properties of novel radical adducts **2**• and **3**• by introducing two and three carbazolyl moieties in the triphenylmethyl core. In addition, we have prepared radical adducts **5**•−**7**• with large octanoyl chains in the 3- and 6-positions of the carbazolyl moiety of **1**•−**3**•. Two of them, adducts **5**• and **6**• form real amorphous glasses.

## Results and Discussion

**Synthesis.** Scheme 1 illustrates the procedures used for the preparation of radical adducts **2**• and **3**•. The method and conditions of the processes to obtain **2**• and **3**•, starting from **1**• and **2**•, respectively, are similar to those used to obtain **1**• from TTM radical.[6] Therefore, radical **1**• with an excess of carbazole in the presence of the appropriate base, cesium carbonate, in boiling dimethylformamide (DMF), followed by hydrolysis with an excess of diluted hydrochloric acid, gave a mixture of the corresponding biscarbazolyltriphenylmethane **2**, with moderate yield, and carbazolyltriphenylmethane **1**, product of the reduction of **1**•. In a similar way, triscarbazolyltriphenylmethane **3** was prepared in low yield, together with biscarbazolyltriphenylmethane **2**, from the reaction of radical **2**• with carbazole and cesium carbonate in DMF. Then, **2** and **3** in tetrahydrofuran with an aqueous solution of tetrabutylammonium hydroxide (TBAH) followed by oxidation with 2,3,5,6-tetrachloro-*p*-benzoquinone gave pure adducts **2**• and **3**•, respectively. The formation of the reduced compounds **1** and **2** as byproduct in the reactions starting from **1**• and **2**•, respectively, with carbazole as reactive, suggests that some sort of radical mechanism is operative in these reactions. In fact, the diamagnetic compounds **1** and **2** with carbazole in the same conditions did not react, recovering them in quantitative yields. Consequently, it seems that carbazole in basic medium is oxidized to the carbazolyl radical by electron transfer to **1**• and **2**• to give the charged species $\mathbf{1}^-$ and $\mathbf{2}^-$, respectively, while the carbazolyl radical couples with another molecule of **1**• and **2**• to form the diamagnetic species **2** and **3**, respectively, after further reduction with more carbazole. Then, the charged species $\mathbf{1}^-$ and $\mathbf{2}^-$ yield after acid hydrolysis the corresponding carbazolyltriphenylmethanes **1** and **2**. The reduced species **2** and **3** are also obtained together with the reduced form of TTM radical, tris(2,4,6-

(4) (a) Brunner, K.; van Dijken, A. V.; Borner, H.; Bastiaansen, J. J. A. M.; Kiggen, N. M. M.; Langeveld, B. M. W. *J. Am. Chem. Soc.* **2004**, *126*, 6035–6042. (b) Kuwabara, Y.; Ogawa, H.; Inada, H.; Noma, N.; Shirota, Y. *Adv. Mater.* **1994**, *6*, 6787–679. (c) Koene, B. E.; Loy, D. E.; Thompson, M. E. *Chem. Mater.* **1998**, *10*, 2235–2250. (d) Grigalevicius, S.; Buika, G.; Grazulevicius, J. V.; Gaidelis, V.; Jankauskas, V.; Montrimas, E. *Synth. Met.* **2001**, *122*, 311–314. (e) Grigalevicius, S.; Blazys, G.; Ostrauskaite, J.; Grazulevicius, J. V.; Gaidelis, V.; Jankauskas, V.; Montrimas, E. *Synth. Met.* **2002**, *128*, 127–131. (f) Huang, J.; Niu, Y.; Yang, W.; Mo, Y.; Yuan, M.; Cao, Y. *Macromolecules* **2002**, *35*, 6080–6082. (g) Morin, J. F.; Leclerc, M. *Macromolecules* **2002**, *35*, 8413–8417. (h) Hwang, J.; Sohn, J.; Park, S. Y. *Macromolecules* **2003**, *36*, 7970–7976. (i) Mi, B. X.; Wang, P. F.; Liu, M. W.; Kwong, H. L.; Wong, N. B.; Lee, Ch. S.; Lee, S. T. *Chem. Mater.* **2003**, *15*, 3148–3151. (j) Inomata, H.; Goushi, K.; Masuko, T.; Konno, T.; Imai, T.; Sasabe, H.; Brown, J. J.; Adachi, Ch. *Chem. Mater.* **2004**, *16*, 12851291>(k) Jiang, J.; Jiang, C.; Yang, W.; Zhen, H.; Hung, F.; Cao, Y. *Macromolecules* **2005**, *38*, 4072–4080. (l) Liang, F.; Kurata, T.; Nishide, H.; Kido, J. *J. Polym. Sci. Part A Polym. Chem.* **2005**, *43*, 5765–5773. (m) Sonntag, M.; Kreger, K.; Hanft, D.; Strohriegl, P. Setayesh, S.; de Leeuw, D. *Chem. Mater.* **2005**, *17*, 3031–3039. (n) Gómez-Lor, B.; Henrich, G.; Alonso, B.; Monge, A.; Gutierrez-Puebla, E.; Echavarren, A. M. *Angew. Chem., Int. Ed.* **2006**, *45*, 4491–4494.

(5) (a) Shirota, Y. Recent extensive reviews on the morphological classification of charge-transporting materials are referred in the literature. *J. Mater. Chem.* **2000**, *10*, 1–25. (b) Strohriegl, P.; Grazulevicius, J. V. *Adv. Mater.* **2002**, *14*, 1439–1452. (c) Shirota, Y.; Kageyama, H. *Chem. Rev.* **2007**, *107*, 953–1010.

(6) Gamero, V.; Velasco, D.; Latorre, S.; López-Calahorra, F.; Brillas, E.; Juliá, L. *Tetrahedron Lett.* **2006**, *47*, 2305–2309.

(7) Armet, O.; Veciana, J.; Rovira, C.; Riera, J.; Castañer, J.; Molins, E.; Rius, J.; Miravitlles, C.; Olivella, S.; Brichfeus, J. *J. Phys. Chem.* **1987**, *91*, 5608–5616.

(8) (a) Carilla, J.; Fajarí, L.; Juliá, L.; Riera, J.; Viadel, L. *Tetrahedron Lett.* **1994**, *35*, 6529–6532. (b) Teruel, L.; Viadel, L.; Carilla, J.; Fajarí, L.; Brillas, E.; Sañé, J.; Rius, J.; Juliá, L. *J. Org. Chem.* **1996**, *61*, 6063–6066. (c) Carilla, J.; Fajarí, L.; Juliá, L.; Sañé, J.; Rius, J. *Tetrahedron* **1996**, *52*, 7013–7024. (d) Viadel, L.; Carilla, J.; Brillas, E.; Labarta, A.; Juliá, L. *J. Mater. Chem.* **1998**, *8*, 1165–1172. (e) Domingo, V. M.; Burdons, X.; Brillas, E.; Carilla, J.; Rius, J.; Torrelles, X.; Juliá, L. *J. Org. Chem.* **2000**, *65*, 6847–6855. (f) Carriedo, G. A.; García Alonso, F. J.; Gómez Elipe, P.; Brillas, E.; Juliá, L. *Org. Lett.* **2001**, *3*, 1625–1628. (g) Torres, J. L.; Varela, B.; Brillas, E.; Juliá, L. *J. Chem. Soc., Chem. Commun.* **2003**, 74–75. (h) Gabino, G. A.; García Alonso, F. J.; Gómez Elipe, P.; Brillas, E.; Labarta, A.; Juliá, L. *J. Org. Chem.* **2004**, *69*, 99–104. (i) Jiménez, A.; Selga, A.; Torres, J. L.; Juliá, L. *Org. Lett.* **2004**, *6*, 4583–4586.

(9) Velasco, D.; Castellanos, S.; López, M.; López-Calahorra, F.; Brillas, E.; Juliá, L. *J. Org. Chem.* **2007**, *72*, 7523–7532.

**SCHEME 1**

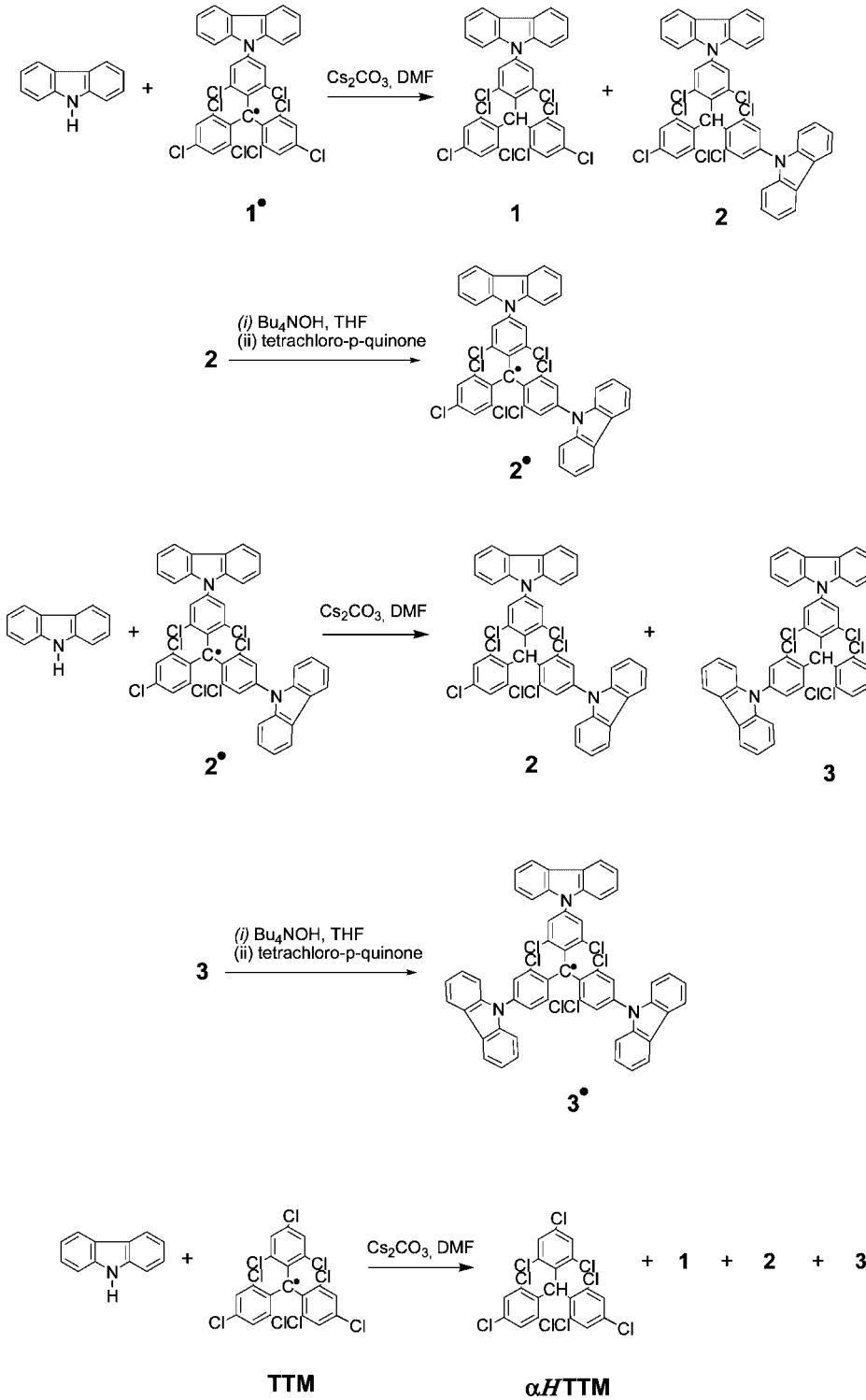


trichlorophenyl)methane (α*H*TTM) in low to moderate yields, in the preparation of **1** from TTM radical with carbazole and cesium carbonate in DMF (Scheme 1).

A Friedel−Craft reaction on radical adduct **1**• with acetyl chloride in carbon disulfide in the presence of $AlCl_3$ leads to radical adduct **4**•[9] with an excellent yield, without impairment of the radical character of the molecule. This excellent result allowed the opportunity to introduce longer alkyl chains at the C-3 and C-6 positions of the carbazole moiety not only on radical adduct **1**•, but also on adducts **2**• and **3**• . Therefore, **1**•, **2**• and **3**• with octanoyl chloride in similar conditions afforded radical adducts **5**•, **6**•, and **7**•, respectively, with excellent and good yields (Chart 1).

The thermal properties of the carbazolyl conjugated radicals **1**•−**7**• were measured by thermogravimetric analysis (TGA) and differential scanning calorimetry (DSC) (for dynamic DSC diagrams of these adducts, see Figures S1−S6 in Supporting Information). Compounds **1**•−**4**• are crystalline colored solids, stable in solid state and in solution. They exhibit a clear endothermic and high melting peak overlapped by an exothermic

**CHART 1**

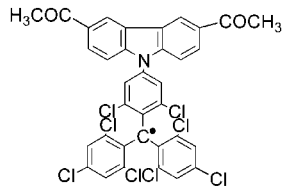

**4•**

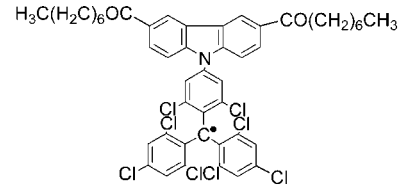

**5•**

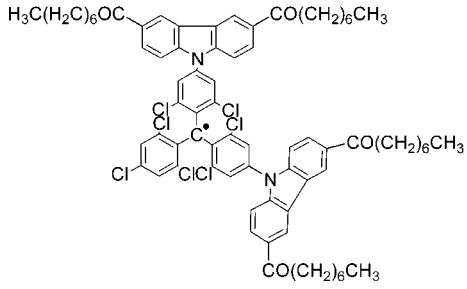

**6•**

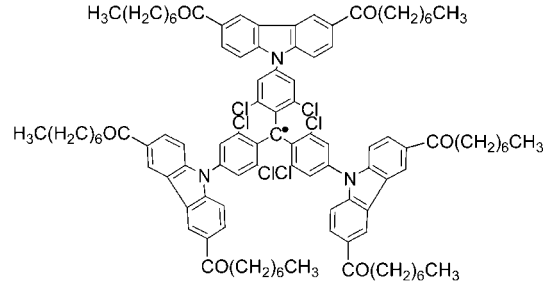

**7•**

**TABLE 1. Melting Points of Radical Adducts 1•− 7• by DSC**

| | mp (°C) | | mp (°C)/dec (°C) |
|---|---|---|---|
| **1•** | 298 dec | **5•** | 188/299 |
| **2•** | 347 dec | **6•** | 143/294 |
| **3•** | 355 dec | **7•** | 249 (292) |
| **4•**[a] | 359 dec | | |

[a] See ref 9.

peak of decomposition at temperatures ≥300 °C. The introduction of large alkyl chains in the carbazole moiety to render radical adducts **5•**−**7•** lowers considerably the melting point of these species moving away from their decomposition temperatures (Table 1), being stable in the melting state in a wide range of temperatures and allowing to form amorphous glasses on cooling, in the case of radicals **5•** and **6•**. Figure 1 shows the heat flow curves of **5•** and **6•** with the temperature up to the melting temperature. They are initially crystalline in the solid state and exhibit a clear endothermic melting peak on first heating without decomposition. When the melted samples are cooled down (10 °C $min^{-1}$), they do not reveal a recrystallization exothermic process, forming stable glasses. In a second heating cycle, samples show a glass transition temperature at 67 and 56 °C, respectively, although they do not crystallize at higher temperatures and the glasses smoothly transform to liquids. It is noticeable to mention that the radical **7•** melts at much higher temperature and is stable in the liquid phase in a very short-range of temperatures (see Table 1 and Figure 2).

**Electron Paramagnetic Resonance.** X-band EPR spectra of the carbazolyl conjugated radicals **1•**−**7•** were recorded in $CH_2Cl_2$ solution (∼ $10^{-3}$ M) at 298 ± 3 K and 160 ± 5 K (adducts **5•**−**7•**, Figure 3 and adducts **1•**−**4•**, Figures S7−S9 in the Supporting Information), and their spectral data are reported in Table 2. In all cases, $g$ values are similar and very close to that of the TTM radical ($g$ = 2.0034 ± 0.0002) and of the free electron ($g_e$ = 2.0023), in agreement with the expected small spin−orbit interaction. All of the spectra at room temperature consisted of a broad and single line, along with a small equidistant pair of lines in both sides of the main spectrum. This small pair corresponds to the strong coupling of the free electron with the α-$^{13}$C nucleus and its values are listed in Table 2. At low temperature, the spectra showed an overlapped multiplet of seven very close lines corresponding to the weak coupling with the six equivalent aromatic hydrogens in meta positions and two weak multiplets in both sides of the central multiplet attributed to the coupling with the three bridgehead-$^{13}$C nuclei adjacents to the α-carbon atom. These couplings, reported in Table 2, are estimated values since it is hard to obtain exact values by spectral simulation when the signals are relatively broad. One can remark that the peak-to-peak line width ($\Delta H_{pp}$) of the different spectra at low temperature increases with

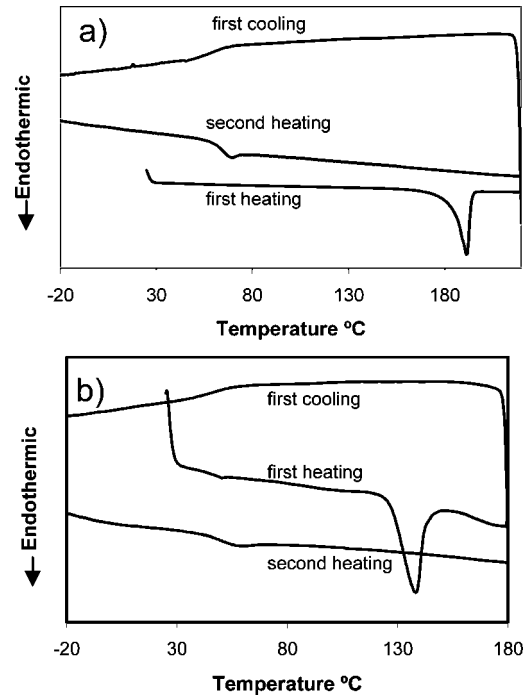


**FIGURE 1.** Thermal analysis results using differential scanning calorimetry: (a) radical adduct **5•**; (b) radical adduct **6•**. (Heating and cooling rate: 10 °C/min).

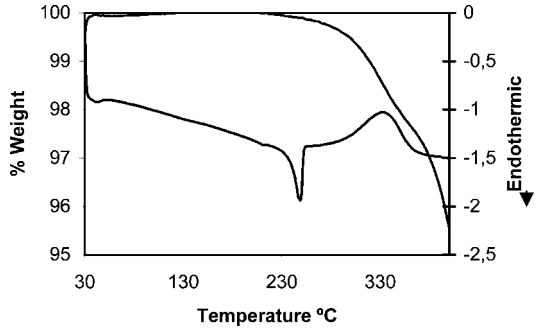


**FIGURE 2.** Thermal analysis (TG and DSC) of radical adduct **7•**. (Heating temperature: 10 °C/min).

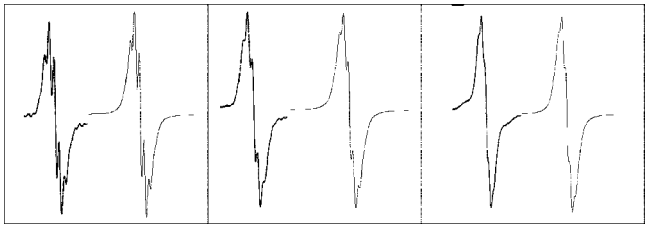

**FIGURE 3.** Black: EPR spectra of radical adducts **5•**−**7•** in $CH_2Cl_2$ solution (∼$10^{-3}$ M) at 160 ± 5 K; modulation amplitude, 0.1. Left: **5•**. Middle: **6•**. Right: **7•**. Blue: Computer simulation.

**TABLE 2. *g* Values and Hyperfine Coupling Constants (Gauss) for Radical Adducts 1•−7• in $CH_2Cl_2$ (∼$10^{-3}$ M)[a]**

| adduct | $g^b$ | 1H | $^{13}C(\alpha)^c$ | $^{13}C(arom)^c$ | $\Delta H_{pp}$ |
|---|---|---|---|---|---|
| **1•**[d] | 2.0032 | 1.25 | 28.0 | 9.0 | 0.80 |
| **2•** | 2.0029 | 1.25 | 28.2 | 9.9 | 0.80 |
| **3•** | 2.0028 | 1.25 | 27.75 | 10.1 | 0.85 |
| **4•**[e] | 2.0032 | 1.25 | 27.90 | 10.5 | 0.65 |
| **5•** | 2.0039 | 1.25 | 26.75 | 10.5 | 0.95 |
| **6•** | 2.0026 | 1.25 | 27.25 | 10.5 | 1.1 |
| **7•** | 2.0029 | 1.25 | 28.75 | 10.5 | 1.2 |

[a] The hfc constants for six 1H in meta and $^{13}C$(arom) (adjacent to α-carbon) and values for $\Delta H_{pp}$ (peak to peak line width) were determined at 180 ± 5 K and checked by computer simulation. [b] *g* values are measured against dpph (2.0037 ± 0.0002) at 298 K. [c] Natural abundance of $^{13}C$ isotope: 1.10%. [d] Values taken from ref 6. [e] Values taken from ref 9.

the number of carbazole moieties in the molecule. $\Delta H_{pp}$ may be at least in part a consequence of the coupling between the free electron and the nitrogen, since it is low enough not to infer additional splittings in the spectra. However, the $\Delta H_{pp}$ values for the spectra of **1•**−**3•** denote practically no variation with the increase of carbazole moieties (see Table 2), and hence, the increase of $\Delta H_{pp}$ in **5•**−**7•** must be related with the slow tumbling rates of the molecules in the solvent, which depend on their size and shape.

The spectrum of a microcrystalline sample of adducts **5•** and **6•** displays a sole line with $\Delta H_{pp}$ of 4.7 and 3.4 G, respectively. When the samples are heated to their melting point for 10 min and then cooled to room temperature to amorphous glasses, their $\Delta H_{pp}$ values become of 2.7 and 5.0 G, respectively (Figure 4). It is assumed that the spectrum of a polyoriented paramagnetic sample, either microcrystalline or amorphous, is made up of a broad envelope of homogeneously peaks from spins resonating at different frequencies, each associated with a certain orientation. This is a consequence of the anisotropic Zeeman and hyperfine interactions. However, there is a small difference in

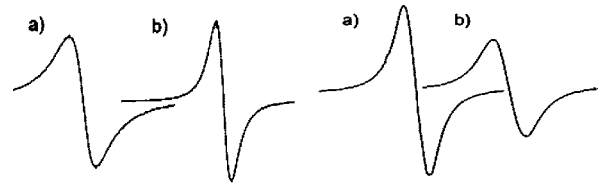


**FIGURE 4.** EPR spectra of radical adducts **5•** (left) and **6•** (right) in two different disordered solid states: (a) microcrystalline state, (b) amorphous state.

**SCHEME 2**

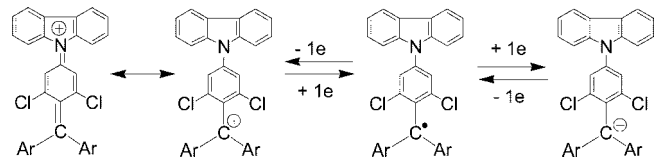


**TABLE 3. Standard Potential for the Redox Pair Related to the Reduction ($O_1/R_1$) and Oxidation ($O_2/R_2$) of Radical Adducts 1•−7•, Difference between Their Anodic ($E_p^a$) and Cathodic ($E_p^c$) Peak Potentials, Electron Affinities, and Ionization Potentials[a]**

| adduct | $E°(O_1/R_1)^b$ (V) $((E_p^a - E_p^c)^c$ (mV)) | $E°(O_2/R_2)^b$ (V) $((E_p^a - E_p^c)^c$ (mV)) | EA (eV) | IP (eV) |
|---|---|---|---|---|
| **1•**[d] | −0.52 (130) | 1.03 (130) | 4.28 | 5.83 |
| **2•** | −0.53 (120) | 0.96 (120) | 4.27 | 5.76 |
| **3•** | −0.52 (90) | 0.90 (80) | 4.28 | 5.70 |
| **4•**[e] | −0.47(130) | 1.18 (140) | 4.33 | 5.98 |
| **5•** | −0.47 (120) | 1.18 (120) | 4.33 | 5.98 |
| **6•** | −0.43 (100) | 1.13 (100) | 4.37 | 5.93 |
| **7•** | −0.39 (90) | 1.12 (100) | 4.41 | 5.92 |

[a] $CH_2Cl_2$ solution (∼$10^{-3}$ M) with $Bu_4NClO_4$ (0.1 M) as background electrolyte on Pt electrode at 25 °C. [b] Potential values versus SCE (saturated calomel electrode). [c] Values at a scan rate of 100 mV $s^{-1}$. [d] Values taken from ref 6. [e] Values taken from ref 9.

the spin-diffusion conditions between microcrystalline and amorphous states. While the spins associated with a particular orientation within each microcrystalline are isolated in space and the magnetization of each microcrystalline develops independently thus minimizing spin diffusion, in the amorphous glassy state all the spins can interact with each other because all the regions overlap and are more sensitive to cross correlation increasing the spin−spin relaxation rate and diminishing the mean lifetime of a given spin-orientation state. In order to preserve the Heisenberg uncertainty principle, the line width of the peak must increase. This is what happens with the spectrum of the adduct **6•** and, surprisingly the contrary occurs for adduct **5•**. So, on going from microcrystalline to amorphous state causes narrowing of the peak of adduct **5•** and broadening of that of adduct **6•**.

**Electrochemical Studies.** Cyclic voltammograms of radical adducts **1•**−**7•** were recorded in $CH_2Cl_2$ solution (∼$10^{-3}$ M) containing tetrabutylammonium perchlorate (0.1 M) as supporting electrolyte on a platinum disk as working electrode at 25 °C using a three-electrode two-compartment cell with a saturated calomel electrode (SCE) as reference electrode and a platinum wire as counter electrode. The voltammograms of each radical displayed two quasi-reversible redox pairs, one corresponding to its reduction ($O_1/R_1$) and the other one to its oxidation ($O_2/R_2$), which are attributed to the equilibrium reactions involving the addition/removal of one electron to/from the trivalent central carbon atom to form its stable anion and cation, respectively. Both redox processes are represented in

**TABLE 4. UV−vis Absorption Data of the Spectra of Radical Adducts 1•−7•, TTM Radical, and 9-Phenylcarbazole (Phcz) in $CHCl_3$**

| adduct | $\lambda_{max}$ (nm) ($\epsilon$)[a] | adduct | $\lambda_{max}$ (nm) ($\epsilon$)[a] |
|---|---|---|---|
| **1•** | 291 (14400); 324 (6870); 339 (9570); 374 (25600); 446 (sh) (2630); 561 (sh) (2130); 598 (2940) | **5•** | 373 (32400); 438 (sh) (4400); 536 (sh) (2000); 567 (1900) |
| **2•** | 292 (28000); 323 (10300); 337 (12200); 376 (22100); 445 (7350); 566 (3750); 609 (5130) | **6•** | 375 (21500); 438 (9600); 542 (sh) (3000); 581 (3500) |
| **3•** | 291 (36200); 323 (12700); 337 (14100); 377 (20500); 454 (13100); 572 (sh) (4920); 614 (7000) | **7•** | 378 (20100); 446 (14200); 550 (sh) (4100); 593 (5450) |
| **4•**[b] | 293 (18800); 328 (20400); 373 (27900); 543 (1840); 559 (1840) | **Phcbz** | 286 (11000); 293 (12600); 326 (2500); 340 (2800) |
| **TTM** | 371 (35000); 494 (635); 539 (700) | | |

[a] Units: $dm^3\ mol^{-1}\ cm^{-1}$. [b] Values taken from ref 9.

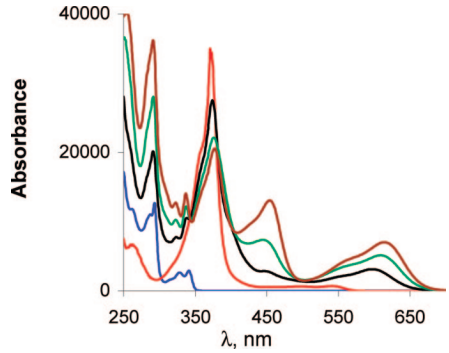


**FIGURE 5.** UV−vis spectra of radical **1•** (black), **2•** (green), **3•** (brown), TTM (red), and 9-phenylcarbazole (blue) in $CHCl_3$.

Scheme 2, also showing the additional stabilization of the cation species by the presence of the heteroatom in the para position relative to the trivalent carbon.[10] Values of the electrochemical parameters are shown in Table 3 (voltammograms are shown in Figures S10−S21, Supporting Information). Each redox process, either in the cathodic or anodic region, is quasi-reversible because the difference between their anodic and cathodic peak potentials is always higher than the theoretical value of 59.2 mV expected for a one-electron reversible process and increases gradually as rising scan rate. Its standard potential ($E°$) was determined as the average of the anodic ($E_p^a$) and cathodic ($E_p^c$) peak potentials. An analysis of Table 3 indicates that by increasing the number of carbazole units in **1•−3•** the standard oxidation potentials become smaller, while no significant variation is denoted in the reduction potentials. On the other hand, as the carbazole substituents, the octanoyl chains, present electron-withdrawing effect, the oxidation potentials of **5•−7•** are shifted to more positive values by comparison with those of **1•−3•**, and the reduction potentials move to less negative values. In general, the electron-withdrawing substituents at the carbazole ring in these radical adducts stabilize the SOMO orbital and, consequently, the ionization potential (IP) and electron affinity (EA) values[11] in **5•−7•** become higher than in **1•−3•**, as can be seen in Table 3.

**Photophysical Properties.** The UV−vis absorption spectra of radical adducts **1•−3•** and **5•−7•** were recorded in $CHCl_3$ solution at concentrations about $10^{-4}$ M. Table 4 summarizes the absorption bands and molar absorptivities of all them along with those of 9-phenylcarbazole and TTM radical. Figure 5 presents the combined absorption spectra of **1•−3•**, TTM radical, and 9-phenylcarbazole. The band at about 290 nm derives from carbazole-centered transition, and the absorption region from 370 to 600 nm is associated with the radical character of these compounds. The band at about 370 nm in **1•−3•** is characteristic of the $\pi-\pi^*$ transition and have features similar to that of TTM radical corresponding to the triphenylmethyl moiety, although the molar absorption coefficients decrease going from **1•** to **3•**. In the range 370−500 nm, the spectra of **1•−3•** exhibit the presence of a new absorption band ($\lambda_{max}$ ~450 nm) bathochromically shifted relative to the $\pi-\pi^*$ transition in the TTM radical ($\lambda_{max}$ ~370 nm), which may be attributed to the contribution of carbazole units. Thus, this band is slightly red-shifted and increases in intensity with the number of carbazole units in the molecule. The lowest-energy range in the visible region between 500−670 nm presents a broadband and a shoulder on the left-side of the peak. The shoulder could correspond to the weak and structured band in TTM radical ($\lambda_{max}$ ~540 nm) being bathochromically shifted in **1•−3•** due to the influence of carbazole moieties. The broad and more intense peak at longer wavelengths shifts from blue to red and increases in intensity following the order **1•** < **2•** < **3•** and can be attributed to a weak charge-transfer band. This feature suggests a partial intramolecular electron transfer in the molecule from the donor, the carbazole moiety, to the acceptor, the trivalent carbon. The spectra of the adducts **5•−7•** (Figure S35, Supporting Information) are similar to those of their unsubstituted parent compounds in the range 250−700 nm. However, it is worth mentioning that all of the absorption maxima except that of the first $\pi-\pi^*$ transition ($\lambda_{max}$ ~370 nm) appear at a slightly shorter wavelength (see Table 4), indicating that the octanoyl groups in the carbazole ring exert an appreciable electron-withdrawing effect.

The visible emission properties of all synthesized radical adducts have been also investigated and are reported in Table 5. The luminescence spectra in diluted solution of cyclohexane and chloroform are depicted in Figure 6. When excited into the visible range of the spectrum ($\lambda_{exc}$ = 450 nm), **1•−7•** showed emission in the range 606−645 nm with cyclohexane as solvent and in the range 618−680 nm with chloroform. It is interesting to remark the considerable red-shift and the large increase in the Stokes shift value ($\Delta S$ ~1245 $cm^{-1}$, see Table 5) in the emission of **1•** on going from a dilute solution in cyclohexane, a nonpolar solvent, to chloroform. This fact provides evidence of the different electronic structure and geometry of the molecule in the excited and ground states. As said above, the absorption spectrum of **1•** suggests the presence of a weak intramolecular charge-transfer in the ground state, this fact being consequently magnified in the excited-state and also confirmed by the dramatic decrease in the quantum yield of the emission in chloroform. In this context, it is known that the fluorescence efficiency in the intramolecular charge transfer states decreases with increasing strength of the transfer, and this is more significant in polar

(10) This additional stabilization is corroborated by the fact that the redox potentials for the oxidation of radicals **1•−7•** are lower than the redox potential of TTM radical ($E°$ = 1.27 V; see ref 9).

(11) EA and IP values for radical adducts **1•−7•** are estimated from the standard potentials of the $O_1/R_1$ and $O_2/R_2$ pairs, respectively, taking a value of −4.8 eV as the SCE energy level relative to the vacuum level.

**TABLE 5. Photophysical Data for Radical Adducts 1•−7•**

| adduct | solvent | $\lambda_{abs}$[a](nm) | $\lambda_{em}$(nm) | $\Phi_F$[b] | Stokes shift ($cm^{-1}$) | $\Delta S$[c] ($cm^{-1}$) |
|---|---|---|---|---|---|---|
| **1•** | cyclohexane | 599 | 628 | 0.53 | 771 | 1245 |
| | chloroform | 598 | 680 | 0.04 | 2016 | |
| **2•** | cyclohexane | 607 | 651 | 0.54 | 1113 | 601 |
| | chloroform | 609 | 680 | 0.10 | 1714 | |
| **3•** | cyclohexane | 611 | 654 | 0.52 | 1077 | 504 |
| | chloroform | 614 | 680 | 0.07 | 1581 | |
| **4•**[d] | toluene | 578 | 625 | 0.48 | 1301 | 407 |
| | chloroform | 559 | 618 | 0.38 | 1708 | |
| **5•** | cyclohexane | 573 | 606 | 0.51 | 950 | 584 |
| | chloroform | 567 | 621 | 0.46 | 1534 | |
| **6•** | cyclohexane | 585 | 621 | 0.56 | 991 | 373 |
| | chloroform | 581 | 631 | 0.49 | 1364 | |
| **7•** | cyclohexane | 597 | 631 | 0.48 | 902 | 244 |
| | chloroform | 598 | 642 | 0.45 | 1146 | |

[a] The less energetic band in the absorption spectra. [b] Quantum yield of luminescence. [c] Difference between Stokes shift in chloroform and cyclohexane. [d] Radical adduct insoluble in cyclohexane. Values taken from ref 9.

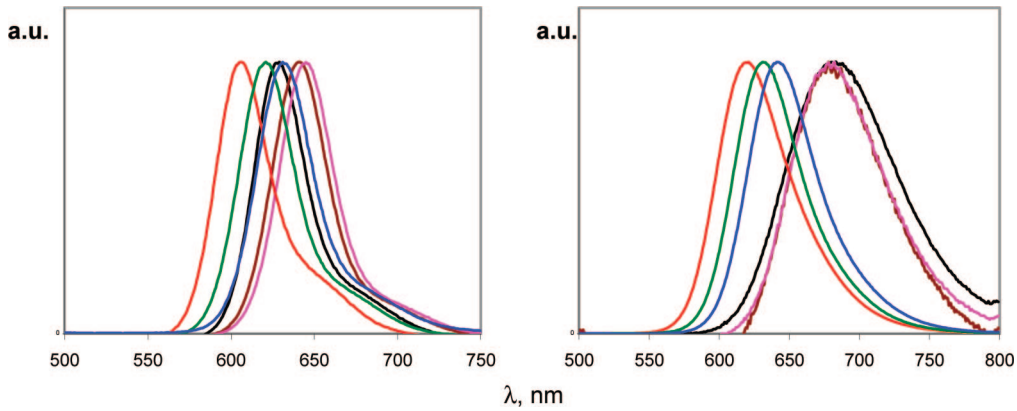


**FIGURE 6.** Normalized fluorescence emission spectra of radical adducts recorded in (left) cyclohexane solution: **1•**, black; **2•**, brown; **3•**, purple; **5•**, red; **6•**, green; **7•**, blue; (right) chloroform solution: **1•**, black; **2•**, brown; **3•**, purple; **5•**, red; **6•**, green; **7•**, blue; at room temperature.

solvents.[12] The smaller red-shift and the lower differences in the Stokes shift values from the emission spectra of **2•** and **3•** from cyclohexane to chloroform ($\Delta S$ ) relative to that of **1•** indicates that the polar nature of the excited states diminishes with the presence of two and three carbazolyl moieties. This behavior is probably by symmetry reasons, a consequence of the greater dispersion of the positive charge in the excited state with the presence of two and three electron-donor carbazolyl moieties in the molecule.

In all cases, emission from acyl-substituted radicals **5•**−**7•** is blue-shifted relative to their parent adducts **1•**−**3•**. It is worth mentioning that the emission intensities of the excited states of **5•**−**7•** in dilute chloroform solution relative to those in cyclohexane are not dramatically diminished, as occurs in **1•**−**3•**. Quantum yields of the emission of **5•**−**7•** are practically equal in both solvents irrespective of the solvent polarity. The different behavior in the emission spectra of radical adducts **5•**−**7•** is due to the presence of the alkylcarbonyl substituents in the carbazole ring and evidence the significant perturbation that these electron-withdrawing substituents exert in the electron-donating capacity of the carbazole moiety.

## Conclusions

We have synthesized two stable radical adducts, **2•** and **3•**, derived from TTM radical with two and three carbazole moieties as substituents at the para positions of the triphenylmethyl group. These syntheses have been performed in the same reaction conditions as the synthesis of **1•**. The substitution of one, two, and three chlorine atoms in the TTM radical by the carbazole group is possible due to the radical character of the molecule. Since these adducts remain stable up to their melting points, decomposing at the melting temperature, large acyl chains have been introduced at the 3- and 6-positions of the carbazole moieties, synthesis of the stable radical adducts **5•**−**7•**, to lower their melting and to provide of a temperature range between the melting and the decomposition temperatures. On the other hand, the presence of the large acyl chains increases the solubility of these species in organic solvents. Two of them, **5•** and **6•** readily form stable amorphous glasses above room temperature although the glass-transition temperatures are low (below 70 °C). The presence of two redox processes in these radical adducts, one of them in the anodic region and the other in the cathodic one, suggests that they have excellent electrochemical stability and exhibit electrochemical amphotericity, being oxidized and reduced indistinctly. UV−vis spectra show the bands associated with the carbazolyl group and with the radical character of these adducts, the later being typical of the absorptions found in the stable radicals of the TTM radical series. In addition, a charge-transfer band more pronounced in adducts **1•**−**3•** than in **4•**−**7•** emerges on the lowest-energy range of the visible spectrum. All of the radical adducts show very

(12) Jenekhe, S. A.; Lu, L.; Alam, M. M. *Macromolecules* **2001**, *34*, 7315–7324.

significant luminescence properties, covering the red spectral band of the emission.

Adducts **5**• and **6**• exhibit two essential properties as candidates to electroluminescent devices: they are amorphous glasses and red fluorescents. Utilization of them as organic semiconductive materials is currently in progress in our laboratory. It is worth mentioning that only very recently, Nishide et al. have reported the first hole transporting molecules based on unpaired electrons, a combination of triarylamines with nitroxide radicals.[13] We focus also our attention in the synthesis of new glassy carbazolylTTM radical adducts with different side chain patterns in the carbazolyl moiety to increase the glass-transition temperature.

## Experimental section

**[4-(*N*-Carbazolyl)-2,6-dichlorophenyl]bis(2,4,6-trichlorophenyl)-methyl Radical (1•) and Bis[4-(*N*-carbazolyl)-2,6-dichlorophenyl](2,4,6-trichlorophenyl)methyl Radical (2•).** A mixture of carbazole (0.500 g; 3.0 mmol), **1**• (0.500 g; 0.73 mmol), anhydrous $Cs_2CO_3$ (0.541 g; 1.6 mmol) and DMF (9 mL) was stirred at reflux (2.75 h) in an inert atmosphere and in the dark. The resulting mixture was poured into an excess of diluted aqueous HCl acid, and the precipitate was filtered off. The solid was chromatographed in silica gel with hexane/$CHCl_3$ (5:1) to give [4-(*N*-carbazolyl)-2,6-dichlorophenyl]bis(2,4,6-trichlorophenyl)methane (**1**) (0.246 g; 49%) [IR (KBr) 3058 (w), 1598 (s), 1576 (s), 1541 (s), 1494 (m), 1478 (m), 1465 (s), 1452 (s), 1442 (m), 1370 (s), 1334 (m), 1314 (m), 1232 (s), 1173 (m), 1142 (m), 1076 (m), 998 (m), 928 (m), 899 (m), 861 (s), 838 (m), 808 (s), 748 (s), 722 (s) $cm^{-1}$; $^1H$ NMR (400 MHz, $CDCl_3$) $\delta$ 8.13 (d, 2H, $J = 6$ Hz), 7.61 (d, 1H, $J = 1.6$ Hz), 7.48 (d, 1H, $J = 1.6$ Hz), 7.44−7.46 (m, 4H), 7.43 (d, 1H, $J = 1.6$ Hz), 7.40 (d, 1H, $J = 1.6$ Hz), 7.30−7.33 (m, 3H), 7.28 (d, 1H, $J = 1.6$ Hz), 6.85 (s, 1H) (see Figure S22, Supporting Information)] and bis[4-(*N*-carbazolyl)-2,6-dichlorophenyl](2,4,6-trichlorophenyl)methane (**2**) (0.220 g; 37%): IR (KBr) 3058 (w), 1598 (s), 1576 (s), 1543 (s), 1493 (s), 1479 (m), 1464 (s), 1452 (s), 1442 (m), 1334 (m), 1310 (m), 1228 (s), 1174 (m), 1074 (m), 998 (m), 921 (m), 884 (m), 878 (m), 831 (m), 797 (s), 748 (s), 721 (s) $cm^{-1}$; $^1H$ NMR (400 MHz, $CDCl_3$) $\delta$ 8.14 (d, 4H, $J = 6.4$ Hz), 7.68 (d, 1H, $J = 1.6$ Hz), 7.65 (d, 1H, $J = 1.6$ Hz), 7.55 (d, 1H, $J = 1.6$ Hz), 7.52 (d, 1H, $J = 1.6$ Hz), 7.45−7.50 (m, 10 H), 7.35−7.32 (m. 6H), 7.03 (s, 1H) (see Figure S23, Supporting Information). Anal. Calcd for $C_{43}H_{23}Cl_7N_2 \cdot {}^1/_5CHCl_3$: C, 61.8; H, 2.8; Cl, 32.1; N, 3.3. Found: C, 61.7; H, 2.8; Cl, 31.5; N, 3.3.

An aqueous solution of TBAH (1.5 M) (2 mL; 3.0 mmol) was added to a solution of **1** (1.453 g; 2.1 mmol) in THF (45 mL) and stirred (5 h) in an inert atmosphere at rt, and then tetrachloro-*p*-benzoquinone (1.41 g; 5.7 mmol) was added. The solution was stirred in the dark (45 min) and evaporated to dryness, giving a residue which was filtered through silica gel with hexane to give **1**• (1.203 g; 83%): mp (DSC) 298 °C dec; UV ($CHCl_3$) $\lambda_{max}$/nm ($\epsilon$/L $mol^{-1}$ $cm^{-1}$) 291 (14400), 324 (6900), 339 (9600), 374 (25800), 446 (2600), 564 (sh) (2100), 598 (2940); EI-HRMS calcd for $C_{31}H_{14}Cl_8N$ 679.863446, found *m*/*z* 679.862383.

An aqueous solution of TBAH (1.5 M) (1.25 mL; 1.87 mmol) was added to a solution of **2** (0.685 g; 0.8 mmol) in THF (30 mL) and stirred (5.25 h) in an inert atmosphere at rt, and then tetrachloro-*p*-benzoquinone (1.10 g; 4.4 mmol) was added. The solution was stirred in the dark (2.5 h) and evaporated to dryness, giving a residue which was filtered through silica gel with $CHCl_3$ to give **2**• (0.640 g; 93%): mp (DSC) 347 °C dec; IR (KBr) 3053 (w), 1573 (s), 1524 (m), 1493 (s), 1471 (s), 1341 (m), 1333 (s), 1310 (m), 1226 (m), 804 (m), 748 (s), 720 (m) $cm^{-1}$; UV ($CHCl_3$) $\lambda_{max}$/nm ($\epsilon$/L $mol^{-1}$ $cm^{-1}$) 292 (28000), 323 (10300), 337 (12200), 376 (22100), 445 (7350), 571 (sh) (3840), 609 (5130); EI-HRMS calcd for $C_{43}H_{22}Cl_7N_2$ 810.960268, found *m*/*z* 810.959629.

**Tris[4-(*N*-carbazolyl)-2,6-dichlorophenyl]methyl Radical (3•).** A mixture of carbazole (0.500 g; 3.0 mmol), **2**• (0.500 g; 0.61 mmol), anhydrous $Cs_2CO_3$ (0.500 g; 1.5 mmol), and DMF (10 mL) was stirred at reflux (2.5 h) in an inert atmosphere and in the dark. The resulting mixture was poured into an excess of diluted aqueous HCl acid, and the precipitate was filtered. The solid was chromatographed in silica gel with $CCl_4$ to give bis[4-(*N*-carbazolyl)-2,6-dichlorophenyl](2,4,6-trichlorophenyl)methane (**2**) (0.415 g; 83%), identified by IR and a mixture (0.102 g) which was further separated by thin layer chromatography to give of tris[4-(*N*-carbazolyl)-2,6-dichloro)phenyl]methane (**3**) (0.071 g; 12%): IR (KBr) 3055 (w), 2953 (m), 2923 (m), 2853 (m), 1596 (s), 1574 (m), 1543 (w), 1493 (m), 1463 (s), 1453 (s), 1333 (m), 1310 (m), 1227 (m), 1172 (w), 1151 (w), 1073 (w), 996 (w), 921 (w), 878 (w), 799 (m), 746 (s), 721 (m), 652 (w); $^1H$ NMR (300 MHz, $CDCl_3$) $\delta$ 8.15 (d, 6H, $J = 7.4$ Hz), 7.72 (d, 3H, $J = 2.4$ Hz), 7.59 (d,3H, $J = 2.1$ Hz), 7.53−7.46 (m,12H), 7.37−7.32 (m, 6H), 7.21 (s, 1H) (see Figure S24, Supporting Information). Anal. Calcd for $C_{55}H_{31}Cl_6N_3$: C, 69.8; H, 3.3; Cl, 22.5; N, 4.4. Found: C, 69.8; H, 3.8; Cl, 21.7; N, 4.2.

An aqueous solution of TBAH (1.5M) (0.3 mL; 0.45 mmol) was added to a solution of **3** (0.084 g; 0.09 mmol) in THF (10 mL) and stirred (7 h) in an inert atmosphere at rt, and then tetrachloro-*p*-benzoquinone (0.140 g; 0.6 mmol) was added. The solution was stirred in the dark (1.5 h), left overnight in the dark, and evaporated to dryness, yielding a residue which was filtered through silica gel with $CCl_4$ and dried at low pressure to eliminate the excess of tetrachloro-*p*-benzoquinone to give **3**• (0.050 g; 59%): mp (DSC) 355 °C (dec); IR (KBr) 3065 (w), 1571 (s), 1524 (m), 1493 (m), 1453 (s), 1335 (s), 1312 (m), 1224 (m), 806 (m), 746 (s), 723 (s) $cm^{-1}$; UV ($CHCl_3$) $\lambda_{max}$/nm ($\epsilon$/L $mol^{-1}$ $cm^{-1}$) 291 (36200), 323 (12700), 337 (14050), 377 (20500), 454 (13050), 575 (sh) (4930), 614 (7000); (MALDI-ToF) HRMS calcd for $C_{55}H_{30}Cl_6N_3$ 942.0590, found *m*/*z* 942.0565.

**Reaction of Tris(2,4,6-trichlorophenyl)methyl (TTM) Radical with NH-Carbazole in DMF.** A mixture of carbazole (3.10 g; 18.6 mmol), TTM radical (3.00 g; 5.4 mmol), anhydrous $Cs_2CO_3$ (2.91 g; 8.7 mmol), and DMF (55 mL) was stirred at reflux (2 h) in an inert atmosphere and in the dark. The resulting mixture was poured into an excess of diluted aqueous HCl acid, and the precipitate was filtered off. The solid was chromatographed in silica gel with hexane/$CHCl_3$ (5:1) to give tris(2,4,6-trichlorophenyl)methane (0.886 g; 29%) identified by IR, [4-(*N*-carbazolyl)-2,6-dichlorophenyl]bis(2,4,6-trichlorophenyl)methane (**1**) (1.453 g; 39%), bis[4-(*N*-carbazolyl)-2,6-dichlorophenyl](2,4,6-trichlorophenyl)methane (**2**) (0.716 g; 16%), and tris[4-(*N*-carbazolyl)-2,6-dichloro)phenyl]methane (**3**) (0.144 g; 3%).

**Synthesis of Radicals 4• −7•. General Procedure.** A mixture containing the suitable radical precursor, powdered $AlCl_3$, and carbon disulfide ($CS_2$) was stirred at reflux under phosphorus pentaoxide ($P_2O_5$) atmosphere. Octanoylchloride was added and evolution of gas was observed. After 2−3 h of reaction, the solvent was evaporated and the crude was treated with an ice/water/HCl mixture and extracted with chloroform. The organic layer was dried and evaporated to dryness and the resulting residue was purified.

**[2,6-Dichloro-4-(3,6-dioctanoyl-*N*-carbazolyl)phenyl]bis(2,4,6-trichlorophenyl)methyl Radical (5•).** Starting materials: **1**• (300 mg; 0.44 mmol), $AlCl_3$ (117 mg; 0.88 mmol), octanoyl chloride (0.17 mL; 1 mmol), $CS_2$ (18 mL). Reaction time 2 h. The residue was chromatographed in silica gel with chloroform to give **5**• (367 mg; 89%): mp (DSC) 188 °C; IR (KBr) 3060 (w), 2953 (m), 2925 (s), 2853 (m), 1676 (s), 1594 (m), 1574 (s), 1555(m), 1524 (m), 1479 (m), 1370 (m), 1334 (m), 1290 (m), 1232 (m), 1183 (m), 1137 (m), 924 (m), 858 (s), 814 (s), 798 (s), 724 (m); UV ($CHCl_3$) $\lambda_{max}$/nm ($\epsilon$/L $mol^{-1}$ $cm^{-1}$) 263 (66700), 290 (sh) (36900), 328 (22700), 373 (32400), 438 (sh) (4400), 567 (1900) nm; EI-HRMS calcd for $C_{47}H_{42}Cl_8NO_2$ 932.072377, found *m*/*z* 932.070085.

(13) (a) Suga, T.; Konishi, H.; Nishide, H. *J. Chem. Soc., Chem. Commun.* **2007**, 1730–1732. (b) Kurata, T.; Koshika, K.; Kato, F.; Kido, J.; Nishide, H. *J. Chem. Soc., Chem. Commun.* **2007**, 2986–2988. (c) Kurata, T.; Koshika, K.; Kato, F.; Kido, J.; Nishide, H. *Polyhedron* **2007**, *26*, 1776–1780.

**Bis[2,6-dichloro-4-(3,6-dioctanoyl-*N*-carbazolyl)phenyl](2,4,6-trichlorophenyl)methyl Radical (6•).** Starting materials: **2•** (200 mg; 0.25 mmol), $AlCl_3$ (207 mg; 1.55 mmol), octanoyl chloride (0.26 mL; 1.55 mmol), $CS_2$ (18 mL). Reaction time 3 h. The residue was chromatographed in silica gel with chloroform/hexane (7:3) to give **6•** (296 mg; 90%): mp (DSC) 143 °C; IR (KBr) 3060 (w), 2954 (m), 2928 (s), 2850 (m), 1676 (s), 1624 (m), 1595 (m), 1574 (s), 1526 (m), 1482 (m), 1369 (m), 1338 (m), 1291 (m), 1237 (m), 1189 (m), 818 (m), 806 (m); UV ($CHCl_3$) $\lambda_{max}$/nm ($\epsilon$/L mol$^{-1}$ cm$^{-1}$) 263 (105200), 292 (62800), 327 (38000), 375 (21500), 438 (sh) (9600), 581 (3500) nm; (MALDI-ToF)-HRMS calcd for $C_{75}H_{78}Cl_7N_2O_4$ 1315.3776, found *m*/*z* 1315.3776.

**Tris[2,6-dichloro-4-(3,6-dioctanoyl-*N*-carbazolyl)phenyl]methyl Radical (7•).** Starting materials: **3•** (35 mg; 0.037 mmol), $AlCl_3$ (40 mg; 0.3 mmol), octanoyl chloride (0.05 mL; 0.3 mmol), and $CS_2$ (8 mL). Reaction time: 2 h. The residue was purified by thin-layer chromatography eluting with chloroform to give **7•** (40 mg; 60%): mp (DSC) 249 °C dec; IR (KBr) 3060 (w), 2953 (m), 292 (s), 2851 (m), 1678 (s), 1623 (m), 1593 (m), 1571 (s), 1522 (m), 1476 (m), 1357 (m), 1333 (m), 1287 (m), 1230 (m), 1184 (m), 802 (s); UV ($CHCl_3$) $\lambda_{max}$/nm ($\epsilon$/L mol$^{-1}$ cm$^{-1}$) 263 (142500), 293 (87000), 326 (51800), 378 (20100), 446 (14200), 593 (5450) nm; (MALDI-ToF)-HRMS calcd for $C_{103}H_{114}Cl_6N_3O_6$ 1698.6833, found *m*/*z* 1698.6899.

**Acknowledgment.** Financial support for this research was obtained from the Ministerio de Educación y Ciencia (Spain) through Grant No. CTQ2006-15611-C02-02/BQU. S.C. is gratefully acknowledged to the Generalitat de Catalunya for a predoctoral grant. We also thank the EPR service of the Institut d'Investigacions Químiques i Ambientals de Barcelona (CSIC) for recording the EPR spectra.

**Supporting Information Available:** General experimental procedures, differential scanning calorimeter analysis (Figures S1−S6), EPR spectra (Figures S7−S9), cyclic voltammograms (Figures S10−S21), $^1$H NMR spectra (Figures S22−S24), and IR spectra (Figures S25−S34) for new radical adducts **2•**−**7•** and for new diamagnetic compounds **1**−**3**. This material is available free of charge via the Internet at http://pubs.acs.org.

JO702723K